THE RELATION BETWEEN THE HORIZONTAL WIND FIELD AND HEIGHT TENDENCIES IN AN ISOBARIC SURFACE

ALVIN LEE MORRIS

Artisan Gold Lettering & Smith Bindery

593 - 15th Street Oakland, Calif. GLencourt 1-9827

DIRECTIONS FOR BINDING

BIND IN
(CIRCLE ONE)

BUCKRAM
COLOR NO. 8854

FABRIKOID
COLOR_____

LEATHER
COLOR_____

LETTERING ON ~~BACK~~ shelf TO BE EXACTLY AS PRINTED HERE.

MORRIS

1954

Thesis
M823

OTHER INSTRUCTIONS

Letter in gold.
Letter on the front cover:

THE RELATION BETWEEN THE HORIZONTAL WIND FIELD AND HEIGHT TENDENCIES IN AN ISOBARIC SURFACE

ALVIN LEE MORRIS

THE RELATION BETWEEN THE HORIZONTAL WIND FIELD AND HEIGHT TENDENCIES IN AN ISOBARIC SURFACE

****

Alvin L. Morris

THE RELATION BETWEEN THE HORIZONTAL WIND FIELD AND HEIGHT TENDENCIES IN AN ISOBARIC SURFACE

by

Alvin Lee Morris
Lieutenant Commander
United States Naval Reserve

Submitted in partial fulfillment
of the requirements
for the degree of

MASTER OF SCIENCE
IN AEROLOGY

United States Naval Postgraduate School
Monterey, California

1 9 5 4

This work is accepted as fulfilling

the thesis requirements for the degree of

MASTER OF SCIENCE

IN AEROLOGY

from the

United States Naval Postgraduate School

PREFACE

The purpose of this research was to explore the relation between the horizontal wind field, the isobaric surface configuration and the vertical motion of the isobaric surface.

This work was conducted at the U. S. Naval Postgraduate School, Monterey, California, during the period January to May 1954.

I wish to express my appreciation to Professor F. L. Martin for his advice and guidance throughout this study.

TABLE OF CONTENTS

LIST OF ILLUSTRATIONS
AND TABLES

TABLE OF SYMBOLS AND ABBREVIATIONS

f	- Coriolis parameter ($f = 2\Omega \sin\phi$)
Ω	- Angular speed of earth's rotation
ϕ	- Latitude
K	- Curvature of a trajectory
V	- Wind speed
$\vec{V}$	- Vector wind velocity
g	- Acceleration of gravity
t	- Time
Z	- Height of the isobaric surface
n	- Horizontal coordinate normal to the path increasing to the left
s	- Horizontal coordinate along the path
$\vec{k}$	- Unit vector pointing vertically upward
$\vec{t}$	- Unit tangent vector pointing along the path
$\vec{n}$	- Unit normal vector pointing to the left of the path
∇_H	- Horizontal differential operator
ψ	- Angle between wind vector and east
x	- Horizontal coordinate increasing to the east
y	- Horizontal coordinate increasing to the north
K_s	- Curvature of a streamline
A	- The first term on the right side of Equations (2.6) and (2.9); also called the cross contour term of (2.6) and (2.9)
B	- The second term on the right side of Equations

(2.6) and (2.9); also called the wind difference term of (2.6) and (2.9)

C - The third term on the right side of Equation (2.9)

V_g - Geostrophic wind speed

R_c - Radius of curvature of the contours on an isobaric chart

R_m - Minimum radius of curvature which gradient flow may have with a given isohyptic gradient

K_{max} - Maximum curvature which gradient flow may have with a given isohyptic gradient

Ω_z - Local vertical component of angular speed of the earth

$CAVT$ - Constant absolute vorticity trajectory

CHAPTER I

INTRODUCTION

It has long been recognized by meteorologists that there is an interdependence between the pressure distribution and wind flow on a level surface. In the steady state the pressure, Coriolis and centripetal accelerations all sum vectorially to zero. The steady state is a condition which may be frequently approximated in nature, but it is probably seldom realized. Thus, there is a process of continual adjustment going on in the atmosphere. The wind accelerates in response to changes of pressure gradient, and pressure gradient changes in response to non-gradient winds.

Rossby [8] and Cahn [3] studied the mutual adjustment of pressure and velocity distributions in certain simple current systems. These currents were narrow but infinite in length, having a current profile similar to that which has now become associated with the jet stream.

Unbalanced forces appear to occur in the atmosphere in another important fashion, which has been emphasized recently by O'Connor [6] because of its importance in prognostic analysis. In this situation strong winds are found either upstream

or downstream of light winds. This condition is observed daily between the isotach maxima and minima occurring along the jet stream on the upper-level facsimile charts prepared by the WBAN Analysis Center. Under these circumstances it is easy to see that even though all forces may be balanced at a given instant, inertia may carry air into a region with speeds which are not compatible with the pressure distribution existing there. What occurs then is not well understood, but there must be some mutual adjustment between the wind velocity and the pressure distribution.

Brunt [2] discusses an investigation of this problem by Brunt and Douglas. This treatment of the problem makes a number of simplifications and does not show the effect of the curvature of the air motion. Petterssen [7] discusses this problem in a slightly different manner, but makes the same approximations as Brunt and Douglas. The method of Petterssen is followed and extended in this study, but the equations of motion will be expressed in terms of the topography of an isobaric surface instead of the pressure distribution in a level surface.

All equations and the discussion which follow refer specifically to the Northern Hemisphere.

CHAPTER II

DERIVATION OF THE ISALLOHYPTIC GRADIENT EQUATION

The equations of frictionless horizontal flow on an isobaric surface referred to a natural coordinate system are

$$(f+KV)V = -g\frac{\partial z}{\partial n}$$

and

$$\frac{dV}{dt} = -g\frac{\partial z}{\partial s} \tag{2.1}$$

These may be written in vector form as follows:

$$g\,\mathbb{K}\times\nabla_H z = (f+KV)V\mathbb{t} - \mathbb{n}\frac{dV}{dt} \tag{2.2}$$

Differentiating partially with respect to time, we obtain

$$g\,\mathbb{K}\times\nabla_H\frac{\partial z}{\partial t} = (f+KV)\left(\frac{\partial V}{\partial t}\mathbb{t} + V\frac{\partial \mathbb{t}}{\partial t}\right) + V\left(K\frac{\partial V}{\partial t} + V\frac{\partial K}{\partial t}\right)$$
$$-\mathbb{n}\frac{\partial}{\partial t}\left(\frac{dV}{dt}\right) - \frac{dV}{dt}\frac{\partial \mathbb{n}}{\partial t}$$

Since $\frac{\partial \mathbb{t}}{\partial t} = \mathbb{n}\frac{\partial \psi}{\partial t}$ and $\frac{\partial \mathbb{n}}{\partial t} = -\mathbb{t}\frac{\partial \psi}{\partial t}$,

$$g\,\mathbb{K}\times\nabla_H\frac{\partial z}{\partial t} = \mathbb{t}\left[(f+2KV+\frac{\partial \psi}{\partial t})\frac{dV}{dt} - V\frac{\partial V}{\partial s}(f+2KV) + V^2\frac{\partial K}{\partial t}\right]$$
$$+\mathbb{n}\left[(f+2KV)V\frac{\partial \psi}{\partial t} - \frac{\partial}{\partial t}\left(\frac{dV}{dt}\right)\right]$$

Taking a cross product of both sides with $\mathbb{K}$ gives

$$g\nabla_H\frac{\partial z}{\partial t} = -\mathbb{n}\left[(f+2KV+\frac{\partial \psi}{\partial t})\frac{dV}{dt} - V\frac{\partial V}{\partial s}(f+2KV) + V^2\frac{\partial K}{\partial t}\right] \tag{2.3}$$
$$+\mathbb{t}\left[(f+KV)V\frac{\partial \psi}{\partial t} - \frac{\partial}{\partial t}\left(\frac{dV}{dt}\right)\right]$$

This is a form of the Brunt Douglas equation. The left side, except for the factor g, is the negative of the isallohypotic gradient. No terms have been ignored, and the only assumption thus far is that the motion is horizontal and frictionless.

In this form (2.3) is difficult to evaluate, since every term on the right-hand side involves a time derivative. Other expressions may be obtained which may be substituted for some of these. One of these is obvious from the tangential component of (2.1). Thus $-g\frac{\partial z}{\partial s}$ may be substituted for $\frac{dV}{dt}$ in the first term on the right of (2.3).

This type of direct substitution is not valid in the term $\frac{\partial}{\partial t}\left(\frac{dV}{dt}\right)$, however, since the coordinate system used is not fixed (see Figure 1). In this case

$$\frac{dV}{dt} = -g\frac{\partial z}{\partial s}, \qquad s = s(x, y)$$

and

$$\frac{\partial}{\partial t}\left(\frac{dV}{dt}\right) = -g\frac{\partial}{\partial t}\left(\frac{\partial z}{\partial x}\frac{\partial x}{\partial s} + \frac{\partial z}{\partial y}\frac{\partial y}{\partial s}\right).$$

But $\frac{\partial x}{\partial s} = \cos\psi$ and $\frac{\partial y}{\partial s} = \sin\psi$.

Therefore, $\frac{\partial}{\partial t}\left(\frac{dV}{dt}\right) = -g\frac{\partial}{\partial t}\left(\frac{\partial z}{\partial x}\cos\psi + \frac{\partial z}{\partial y}\sin\psi\right)$

where ψ is the angle between the x axis of a fixed xy coordinate system and the unit vector $\vec{s}$ which is directed along the positive s axis of the natural coordinate system. Throughout this work the x and y axis of the fixed coordinate axis will be directed east and north, respectively. Thus, the angle ψ is the angle between the wind direction and the east.

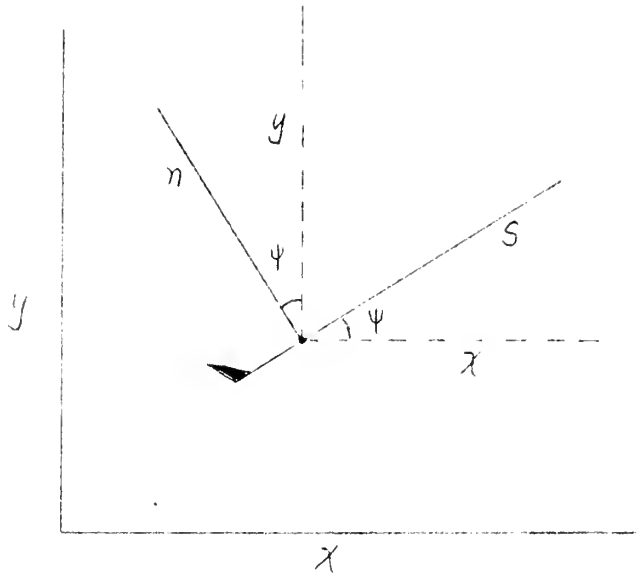

Figure 1.
Coordinate Systems Used in Derivation

Differentiating $\frac{dV}{dt}$ partially with respect to time gives

$$\frac{\partial}{\partial t}\left(\frac{dV}{dt}\right) = -g\left[\frac{\partial^2 z}{\partial x \partial t}\cos\psi + \frac{\partial z}{\partial x}\cos\psi - \frac{\partial z}{\partial x}\sin\psi\,\frac{\partial \psi}{\partial t} + \frac{\partial z}{\partial y}\cos\psi\,\frac{\partial \psi}{\partial t}\right]$$

or

$$\frac{\partial}{\partial t}\left(\frac{dV}{dt}\right) = -g\left[\frac{\partial}{\partial x}\left(\frac{\partial z}{\partial t}\right)\cos\psi + \frac{\partial}{\partial y}\left(\frac{\partial z}{\partial t}\right)\sin\psi - \frac{\partial z}{\partial x}\frac{\partial \psi}{\partial t}\cos\psi + \frac{\partial z}{\partial y}\frac{\partial \psi}{\partial t}\cos\psi\right].$$

This may be written

$$-\frac{\partial}{\partial t}\left(\frac{dV}{dt}\right) = g\frac{\partial}{\partial s}\left(\frac{\partial z}{\partial t}\right) + g\frac{\partial z}{\partial n}\frac{\partial \psi}{\partial t}.$$

The expression on the right may then be substituted for $-\frac{\partial}{\partial t}\left(\frac{dV}{dt}\right)$ in (2.3) and with the direct substitution for $\frac{dV}{dt}$ in the first term on the right side results in

$$g\nabla_n\frac{\partial z}{\partial t} = -\rho\Omega\left[-(f+\zeta)kV + \frac{\partial \psi}{\partial t}\right]g\frac{\partial z}{\partial s} - V\frac{\partial V}{\partial s}(f+\zeta)k + V^2\frac{\partial k}{\partial t}\Big] \qquad (2.4)$$
$$+ \mu\left[\left\{(f+\zeta)V + g\frac{\partial z}{\partial n}\right\}\frac{\partial \psi}{\partial t} + g\frac{\partial}{\partial s}\left(\frac{\partial z}{\partial t}\right)\right]$$

Since the normal component of (2.1) may be written

$$(f+\zeta)V + g\frac{\partial z}{\partial n} = 0$$

it is evident that the term inside braces in (2.4) is zero. Also, the left-hand side of (2.4) may be written in component form as follows:

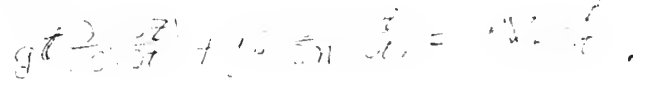

The tangential components of the left and right sides of (2.4) are thus identical, and the right side adds nothing which will assist in evaluating the isallohyptic gradient. While there may be some method of evaluating the tangential component of (2.3) without a direct knowledge of the time rate of change of the acceleration of the wind, it is not obvious. In view of the fact that acceleration is usually ignored in atmospheric motion, it might appear that the term $\frac{\partial}{\partial t}\left(\frac{dV}{dt}\right)$ is negligible. If this is ignored, the tangential component of (2.3) is

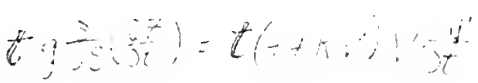

(2.5)

A qualitative interpretation of this equation with reference to the upper air chart (Chapter III) is not too difficult, and an empirical check of it is discussed in Chapter IV.

The normal component of (2.4) is

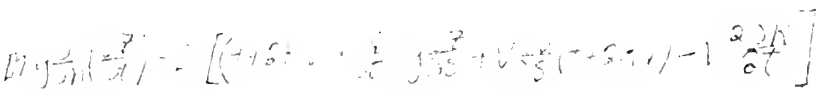

(2.6)

Except for the term involving $\frac{\partial K}{\partial t}$, all terms on the right-hand side of this equation can be evaluated from a synoptic chart. In order to explore the possibility of substituting another expression for $\frac{\partial K}{\partial t}$, Blaton's equation relating trajectory curvature to streamline curvature is recalled.

It may be written $h = h_s + \frac{1}{g}\frac{\partial \psi}{\partial t}$.

From this, taking the derivative with respect to time,

$$\frac{\partial h}{\partial t} = \frac{\partial h_s}{\partial t} + \frac{1}{g}\frac{\partial^2 \psi}{\partial t^2} \quad ;$$

and

$$V\frac{\partial h}{\partial t} = V\frac{\partial h_s}{\partial t} + \frac{V}{g}\frac{\partial^2 \psi}{\partial t^2} \quad . \tag{2.7}$$

Now, $\frac{\partial h_s}{\partial t} = \frac{\partial}{\partial t}(\quad)$ since

$$S = S(x, y)$$

Carrying out the indicated operation gives

$$\frac{\partial h_s}{\partial t} = \quad .$$

This may be written

$$\frac{\partial h_s}{\partial t} = \quad$$

With this substitution, and after some rearrangement (2.7) becomes

$$V\frac{\partial h}{\partial t} = \quad .$$

But

$$\frac{\partial}{\partial t}\left(\frac{\partial \psi}{\partial t}\right) + V\frac{\partial}{\partial s}\left(\frac{\partial \psi}{\partial t}\right) = \frac{d}{dt}\left(\frac{\partial \psi}{\partial t}\right),$$

and

$$\frac{\partial V}{\partial t} = \quad .$$

Therefore,

$$V\frac{\partial h}{\partial t} = V\frac{\partial}{\partial t}\left(\frac{\partial \psi}{\partial t}\right) + V^2\frac{\partial \psi}{\partial n}\frac{\partial \psi}{\partial t} + g\frac{\partial \psi}{\partial t}\frac{\partial z}{\partial s} + V\frac{\partial V}{\partial s}\frac{\partial \psi}{\partial t} \quad . \tag{2.8}$$

Substituting this back in (2.6) yields

$$= \quad .$$

Collecting terms gives

$$\rho g \frac{\partial}{\partial n}\left(\frac{\partial \Psi}{\partial t}\right) = \rho V\left[(f+kV)g\frac{\partial z}{\partial s} + V\frac{\partial V}{\partial s}\left(f+kV-\frac{\partial \Psi}{\partial t}\right) - V\frac{d}{dt}\left(\frac{\partial \Psi}{\partial t}\right) - V^2\frac{\partial \Psi}{\partial t}\frac{\partial \Psi}{\partial n}\right] \tag{2.9}$$

The tangential component of the isallohyptic gradient may be taken in its complete form from (2.3). It is

$$\rho g \frac{\partial}{\partial s}\left(\frac{\partial z}{\partial t}\right) = \rho\left[(f+kV)V\frac{\partial \Psi}{\partial t} - \frac{\partial}{\partial t}\left(\frac{dV}{dt}\right)\right] \tag{2.10}$$

These two equations, (2.9) and (2.10), are the equations for the isallohyptic gradient normal to and along the wind vector, respectively. Equation (2.9) has been put in this form to make numerical evaluation of the equation from the weather map easier. There is some question whether this form is better than (2.6). It is to be noted that as written the units of Equations (2.9) and (2.10) are m sec^{-3}.

CHAPTER III

A QUALITATIVE INTERPRETATION OF THE ISALLOHYPTIC GRADIENT EQUATIONS

Although (2.9) represents the form in which the normal component is evaluated empirically (Chapter IV), it is easier, perhaps, to gain an insight into the meaning of the equation from (2.6).

The term $g\frac{\partial}{\partial n}\left(\frac{\zeta}{f}\right)$, if positive at a given point on an isobaric surface, indicates that, relatively, the isobaric surface is rising more rapidly to the left of the wind direction than to the right. Since the isobaric surface is lower to the left of the wind vector in virtually all instances above the friction layer, a positive value of this term indicates a relaxing isohyptic gradient. Similarly, a negative value of this term can be associated with a tightening isohyptic gradient.

The tangential term $g\frac{1}{f}\left(\frac{\partial \zeta}{\partial t}\right)$ of (2.10) is subject to a similar interpretation. If it is positive, the isobaric surface is rising more rapidly (or falling less rapidly) ahead of the wind vector than behind it. Conversely, if the term is negative, the isobaric surface is falling ahead of the wind vector and rising behind the wind vector relative to the point where the term is being evaluated.

In order to evaluate (2.10), it is necessary to evaluate separately the terms $\left(f+k\zeta\right)V\frac{\partial \Psi}{\partial t}$ and $\frac{\partial}{\partial t}\left(\frac{dV}{n}\right)$. The second term, $\frac{\partial}{\partial t}\left(\frac{dV}{dt}\right)$, is difficult to evaluate, since it is the local rate

of change of acceleration. It is quite small, probably never exceeding 10^{-7} m sec^{-3}. On the other hand, the first term $(f+kV)V\frac{\partial\psi}{\partial s}$ is also quite small. A method for evaluating the latter term numerically is discussed in Chapter IV; however, the sign of this term may be determined by inspection in particular cases.

The factors V and $(f+kV)$ are virtually always positive in the Northern Hemisphere. Thus, the sign of the first term on the right-hand side of (2.10) is determined completely by the sign of the factor $\frac{\partial\psi}{\partial n}$. In a system of progressive open troughs and ridges such as that frequently found on upper-level charts, $\frac{\partial\psi}{\partial t}$ is positive at the ridge line and negative at the trough line. This indicates that on the basis of this term alone, the tangential component of the isallohyptic gradient points in the direction of the wind at the trough line and opposite to the wind at the ridge line, provided the trough and ridge are progressive.

In order for the normal component to be positive, it is necessary that the sum of the three terms on the right-hand side of (2.6) be greater than zero. None of these terms are inherently either positive or negative, and each must be examined carefully in a given situation to determine its sign. These terms will be taken up singly in the following paragraphs to try to determine approximate magnitudes and sign.

Let $A=(f+2\omega V+\frac{\partial\psi}{\partial t})g\frac{\partial z}{\partial s}$ be an abbreviated notation for the first term of (2.6). This term consists of three factors, of which g is the only one which is always positive. The

factor $\frac{\partial Z}{\partial S}$ is positive if the wind is blowing across isohypses toward higher values. The factor f is always positive in the Northern Hemisphere. The wind velocity V is always positive. The curvature K may be positive (cyclonic curvature) or negative (anticyclonic curvature). The term $\frac{\partial \psi}{\partial t}$ may be positive (counterclockwise turning) or negative (clockwise turning). The Coriolis parameter f is of the same order of magnitude as $2KV$, though in most cases it is numerically greater. The term $\frac{\partial \psi}{\partial t}$ is usually not of the same order of magnitude as f, although there are occasional exceptions.

From this one can conclude that the factor $(f+2KV+\frac{\partial \psi}{\partial t})$ will usually be positive. An exception occurs when great anticyclonic curvature is associated with strong winds and the wind is locally turning clockwise with time. No such case has been found in the numerical evaluation of this factor. Thus, the sign of A is usually determined by the cross-contour flow of the wind. This term may vary in magnitude from 0 to 10^{-6} m sec^{-3}.

It is interesting to see what the contribution of this term is under various circumstances. Cross-contour flow toward higher values of Z gives a positive contribution to $\frac{\partial}{\partial n}\left(\frac{\partial Z}{\partial t}\right)$ and indicates a weakening isohyptic gradient. Cross-contour flow toward low values of Z indicates an increasing isohyptic gradient. The reverse of this would occur if $(f+2KV+\frac{\partial \psi}{\partial t})$ were negative, which appears unlikely.

The second term, $B = V\frac{\partial V}{\partial S}(f + 2KV)$, involves the factor $(f + 2KV)$. The variables appearing in this factor have just been discussed. Except for the case of abnormal anticyclonic flow $(V > 2V_g)$, this factor is positive. The velocity, V , is positive always. Therefore, the sign of this entire term is the same as the sign of the factor $\frac{\partial V}{\partial S}$ in nearly all cases.

The sign of $\frac{\partial V}{\partial S}$ is positive if the wind increases along the streamline (i.e. weak winds upstream with strong winds downstream) and negative if the wind is decreasing along the streamline. The magnitude of the term is a function of velocity and rate of change of velocity along the trajectory in an obvious manner. It also is a function of curvature -- strong cyclonic curvature being associated with greater magnitudes, and strong anticyclonic curvature being associated with lower magnitudes.

The term B alone then gives a positive contribution in almost every case when weak winds are moving into an area of strong winds. This is the entrance region of Scherhag [9] . When such an entrance region is associated with cyclonic curvature, the contribution of B is positive and may be relatively large. An entrance region associated with anticyclonic curvature will almost always give a small positive contribution. This difference between the cyclonic and anticyclonic cases is again due to the factor $(f + 2KV)$ of B , discussed above.

When strong winds are moving into a region of weak winds, the term B is nearly always negative. This is the delta region of Sherhag. A delta region associated with cyclonic

curvature results in relatively large negative contributions to $\frac{\partial}{\partial n}\left(\frac{\partial z}{\partial t}\right)$. The contribution of the delta region associated with anticyclonic curvature is negative, but relatively small. In magnitude this term also may vary from 0 to 10^{-6} m sec^{-3}, though it is doubtful that it approaches 10^{-6} very frequently.

The third term on the right-hand side of (2.6) is $C=-V^2\frac{\partial K}{\partial t}$. Thus, if the curvature is increasing locally with time, term C gives a negative contribution. This would occur in a region into which a trough is moving. Conversely, a ridge moving into a region would give a positive contribution to $\frac{\partial}{\partial n}\left(\frac{\partial z}{\partial t}\right)$.

The term C varies in magnitude from 0 to 10^{-7} m sec^{-3}, and appears (See Chapter V) to be generally about one to two orders of magnitude smaller than term A. The range of magnitudes given for all three terms must be considered approximate only.

Several model-type examples are now presented in which, except as noted, only the contributions due to terms A and B are considered. These examples are illustrated in Figure 2.

The first example depicted by Figure 2(a) is a situation in which both terms A and B are positive. It should be noted that the winds, while flowing across contours toward higher values, are stronger downstream than upstream. Therefore, the isallohyptic gradient associated with this must be negative (i.e. $\frac{\partial}{\partial n}\left(\frac{\partial z}{\partial t}\right)$ is positive), and the isohyptic gradient is relaxing.

The curvature of the trajectories does not affect the sign of the isallohyptic gradient in this example unless the trajectory curvature is negative (anticyclonic) and exceeds the critical curvature for gradient flow. This case is discussed below in connection with Figure 2(c). Trajectory curvature does change the magnitude of the isallohyptic gradient however, if all other things are held constant -- cyclonic flow resulting in isallohyptic gradients of greater magnitude than anticyclonic flow.

Figure 2(b) depicts a situation in which terms A and B are both negative. The chief features to be noted are the flow of air across the contours toward the low and the decrease of wind speeds downstream. The isallohyptic gradient associated with this is positive and indicates that the isohyptic gradient is increasing with time. The influence of curvature is precisely the same in this case as for the first case described above.

Figure 2(c) illustrates a condition often found at the crest of a ridge on upper-level charts. The curvature of the contours, given by R_c^{-1}, is negative, but of greater magnitude than the maximum curvature, given by R_m^{-1}, for gradient flow with the existing contour gradient. For this reason, air which is moving over the crest of the ridge will be unable to make the sharp turn required to remain in the contour channel, and so will cross contours toward lower isobaric heights downstream of the ridge. If the trajectory of

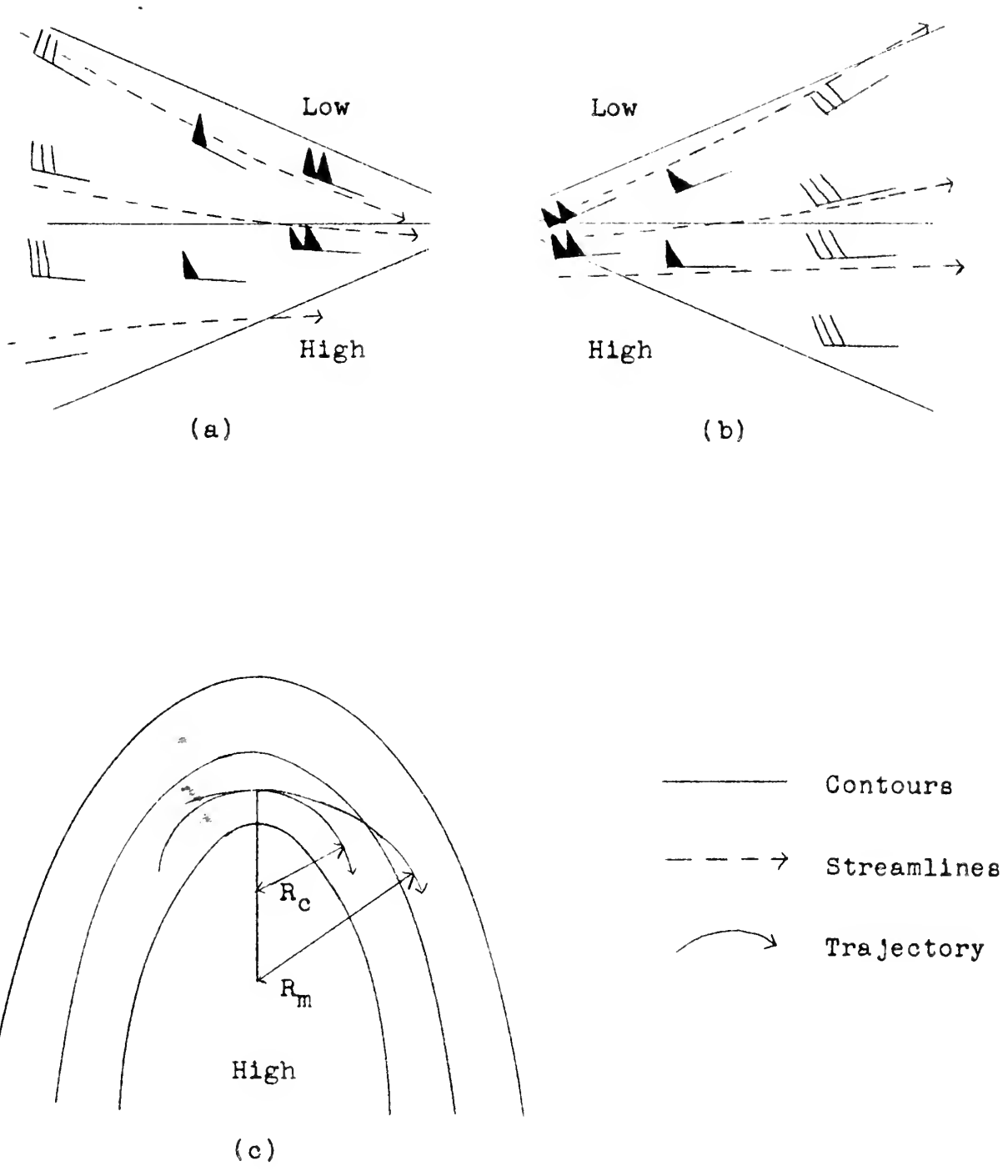

Figure 2. Schematic Illustration of Synoptic Situations for Which Sign of Isallohyptic Gradient May Be Determined by Inspection.

such an overshooting air particle is a trajectory of maximum curvature, then the factor $f+2kV$ is zero. The proof of this statement is given below.

Bjerknes [1] shows that for anticyclonic gradient flow

$$R_m = -\frac{2V_g}{\Omega_z} \quad ; \qquad V = 2V_g$$

Now $\Omega_z = \frac{f}{2}$,

therefore, $R_m = \frac{1}{k_{max}} = -\frac{2V}{f}$.

Hence $f+2k_{max}V=0$.

This condition probably is met occasionally in the situation of Figure 2(c). Then $K = k_{max}$ and (2.6) becomes

$$g\frac{\partial}{\partial n}\left(\frac{\partial z}{\partial t}\right) = g\frac{\partial \psi}{\partial t}\frac{\partial z}{\partial s} - V^2\frac{\partial k}{\partial t} \quad . \qquad (3.1)$$

In this case it is not immediately obvious that the term $V^2\frac{\partial k}{\partial t}$ is small compared with the other terms of the equation, as has heretofore been assumed, nor are the two terms on the right side likely to be of like sign. Indeed, they are likely to give contributions of opposite sign. The factor $\frac{\partial \psi}{\partial t}$ will be positive, and $\frac{\partial z}{\partial s}$ will be negative, resulting in a negative contribution by the first term. The factor $\frac{\partial k}{\partial t}$ will determine the sign of the second term. It will generally be negative, resulting in a positive contribution by the second term. The sign of the isallohyptic gradient, then, is determined by the sign of the term of greater magnitude.

This is a synoptic situation which meteorologists usually agree is accompanied by greater rises of height to the right of the air stream than to the left. These rises take the form of a propagation of the crest of the ridge downstream. Thus, it appears that the negative, or first term on the right of (3.1) is the dominant one. In this example we may have one of the infrequent cases in which $\frac{\partial \psi}{\partial t}$ is of the same order of magnitude as f .

CHAPTER IV

NUMERICAL EVALUATION OF THE ISALLOHYPTIC GRADIENT EQUATIONS

Obtaining general solutions of (2.9) and (2.10) is not, in general, feasible. It is possible, however, to obtain numerical solutions in particular cases, subject to certain simplifying assumptions.

Equation (2.9) may be written in terms of finite differences along a trajectory, as follows:

$$g\frac{\Delta}{\Delta n}\left(\frac{\Delta z}{\Delta t}\right) = \left(f_2 + 2K_2V\right)\rho_2\frac{(z_3 - z_1)}{\Delta s} + V\frac{(V_3 - V_1)}{\Delta s}\left(f_2 + 2K_2V - \frac{\Delta\psi_2}{\Delta t_2}\right)$$
$$- \frac{V}{\Delta t_2}\left(\frac{\Delta\gamma_5}{\Delta t_5} - \frac{\Delta\psi_4}{\Delta t_4}\right) - V^2\left(\frac{\Delta\psi_2}{\Delta t_2}\right)\left(\frac{\psi_6 - \psi_7}{\Delta n}\right) \qquad (4.1)$$

The subscripts refer to points located along a series of trajectories as shown in Figure 3.

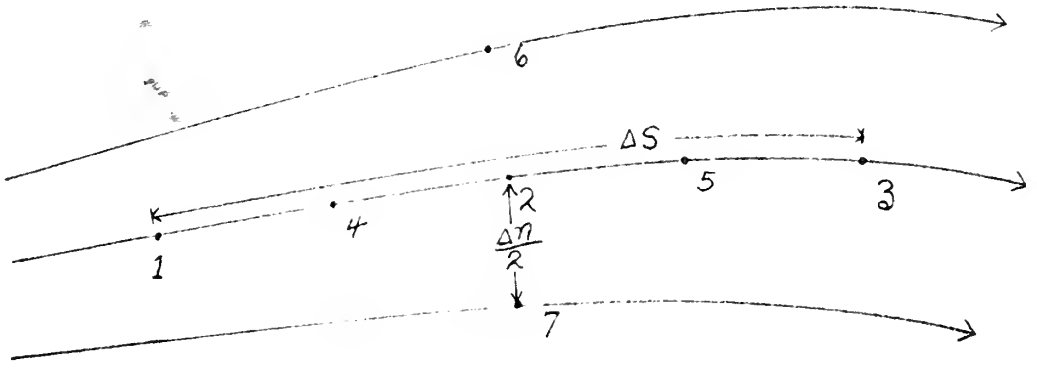

Figure 3. Trajectories Showing the Grid Arrangement Required to Obtain a Numerical Solution of Equations (4.4) and (4.5).

Much of the success of evaluation depends on the accuracy of the trajectories. Because of the fact that adequate upper-air charts are available only at 12-hour intervals, trajectories drawn by the method of successive approximation are of dubious value. Also, these require that the charts be available at both ends of the 12-hour time interval. This makes the result useless as a prognostic tool. It was decided to make use of constant absolute vorticity trajectories (CAVT's) for the numerical work.

The method of constructing CAVT's from inflection points is quite generally known. The assumptions involved (non-divergence, constant lateral shear, frictionless flow, and no vertical motion) are quite restrictive. Equally restrictive for the purposes of this study is the requirement that the CAVT be constructed from an inflection point. Martin [5] in a study which was carried out concurrently with this study pointed out how CAVT's might be constructed from any point. A modification of his method was used in this study and is described in Appendix 1.

The use of a CAVT as the trajectory simplified the evaluation of (4.1) in a number of ways. The arc length ΔS is equal to the product of V and Δt . The curvature, K_2, of the trajectory at point 2 (Figure 3) may be determined from the initial conditions and the latitude of point 2. Also, since the wind direction is known initially, it is a relatively simple matter to determine the turning of the wind at a given

point by measuring the angle between the initial wind direction and a tangent to the CAVT at that point.

Equation (4.1) adapted to the use of 12-hour CAVT's becomes

$$g\frac{\Delta}{\Delta n}\left(\frac{\Delta z}{12}\right)=(f_2+2K_2V)g\frac{(Z_2-Z_1)}{12V}+\frac{V_3-V_1}{12}\left(f+2K_2V-\frac{\Delta\psi_2}{6}\right)$$
$$-\frac{V}{6}\left(\frac{\Delta\psi_5}{4}-\frac{\Delta\psi_4}{3}\right)-V^2\left(\frac{\Delta\psi_2}{6}\right)\left(\frac{\psi_6-\psi_7}{\Delta n}\right). \qquad (4.2)$$

Equation (2.10) written in similar form for numerical evaluation is

$$g\frac{\Delta}{\Delta s}\left(\frac{\Delta z}{12}\right)=(f+K_2V)V\,\frac{\Delta\psi_2}{6}-\frac{\Delta}{12}\left(\frac{\Delta V}{12}\right), \qquad (4.3)$$

The second term on the right in (4.3) cannot be determined, but all other terms in (4.2) and (4.3) may be determined from a set of trajectories like those shown in Figure 3. Equations (4.2) and (4.3) with unit conversions, which permit data taken directly from an analyzed upper air chart to be used without change, become

$$\frac{\Delta}{\Delta n}(\Delta z)=(0.524\sin\phi_2+0.033K_2V)\frac{60(Z_2-Z_1)}{V}$$
$$+0.534(V_3-V_1)\left(0.524\sin\phi_2+0.033K_2V-\frac{\Delta\psi_2}{344}\right)$$
$$-0.208\times10^{-2}V(\Delta\psi_5-3\Delta\psi_4)-5.24\times10^{-6}V^2\Delta\psi_2\left(\frac{\psi_6-\psi_7}{\Delta n}\right), \qquad (4.4)$$

and

$$\frac{\Delta}{\Delta s}(\Delta z)=0.196\left(0.524\sin\phi_2+\frac{KV}{60}\right)V\Delta\psi_2. \qquad (4.5)$$

The difference Δz found on the left side of these equations is the 12-hour change of height of the isobaric surface. The units in which the various parameters are ex-

pressed are as follows: V (knots), K (reciprocal of degrees of latitude), Z (feet), ψ and $\Delta\psi$ (degrees), Δn and ΔS (degrees of latitude). The isallohyptic ascendant is expressed in terms of feet per degree of latitude per 12 hours. All computed and observed values are of the isallohyptic ascendant.

A series of 44 computations were made using CAVT's on the 500 mb. level charts for 0300Z and 1200Z , 12 March 1954 and 0300Z , 13 March 1954. The only criterion used in selecting the points from which the CAVT's were constructed was that initial conditions be as clear-cut as possible. Approximately one-third of the trajectories were started from troughs. One-third were from inflection points on the west side of a trough, and the other one-third were from inflection points east of a trough. The fourth term of the right side of (4.4) proved to be so small that it was ignored.

Another series of 21 computations were made from CAVT's on 500 mb. level charts selected from the period 9 through 18 April 1954. The criterion used in selecting the CAVT starting point was that it be on an isotach maximum. This made the second term on the right in (4.4) negative in every case. All trajectories of both series have starting points within the United States.

The computed normal components of the isallohyptic ascendant are shown for the series of 44, with the observed values, in Table 1. The coefficient of correlation between computed and observed values is + 0.65, indicating that approximately 43% of the observed variation is accounted for by the computed

values. For 44 values the correlation coefficient, +0.65, is highly significant at the 99% level of belief, according to Hoel [4].

The regression equation (Figure 4 shows the scatter diagram and regression line of observed values y on computed values x) is

$$y = 8{,}67 + 0{,}35\,x .$$

In this x and y are expressed in units of feet per degree latitude per 12 hours. This equation indicates that in this series, the computed values were, for the most part, of the right sign, but too great in magnitude. The dominant term in (4.4) was the cross-contour term in most of the computations in this series. An attempt was made to reduce this term empirically by multiplying it by a constant factor. This did not improve the correlation, however.

Table 1 also lists the computed and observed tangential components from this series of 44 trajectories. The correlation coefficient between these data is +0.59, indicating that approximately 35% of the variance of the observed values is accounted for by the computed values. The correlation coefficient in this instance also is highly significant at the 99% level of belief.

The regression equation of observed values on computed values is

$$y = -5{,}31 + 0{,}51\,x .$$

(See Figure 5 for the scatter diagram and plot of this equation.)

TABLE 1

Components of Isallohyptic Ascendant Associated with CAVT's Constructed on a 500 Mb. Chart

Date and Time	Isallohyptic Ascendant (feet per deg lat per 12 hrs) Normal Component Computed	Normal Component Observed	Tangential Component Computed	Tangential Component Observed	Remarks
	+ 53	+ 28	0	- 18	
	+ 140	+ 27	- 46	- 22	From inflec-
	+ 110	+ 21	- 38	- 23	tion point
	+ 79	0	- 37	- 26	southeast to-
	+ 3	- 12	- 8	- 22	ward trough
	+ 120	+ 120	0	0	
0300Z	- 9	0	0	0	From trough
to	- 33	- 78	0	- 35	northeast to-
1500Z	- 15	- 26	0	- 4	ward inflection
12 Mar.	+ 32	- 25	0	- 4	point
1954	+ 24	- 29	- 6	0	
	- 140	0	+ 120	+ 33	
	+ 12	+ 14	- 20	0	From inflec-
	- 97	- 10	+ 110	+ 28	tion point
	- 78	- 21	+ 43	+ 26	northeast to-
	- 44	- 12	+ 32	+ 9	ward ridge
1500Z	+ 170	+ 54	- 51	0	
12 Mar.	+ 180	+ 91	- 120	- 37	From inflec-
to 0300Z	+ 110	+ 67	- 75	- 17	tion point
13 Mar.	+ 100	+ 38	- 78	- 33	southeast to-
1954	+ 30	+ 50	- 14	- 12	ward trough

TABLE 1
(Continued)

Date and Time	Isallohyptic Ascendant (feet per deg lat per 12 hrs) Normal Component Computed	Normal Component Observed	Tangential Component Computed	Tangential Component Observed	Remarks
	+ 85	+ 140	- 40	- 46	
	- 200	- 91	+ 140	- 38	From trough
	- 67	- 45	+ 15	- 91	northeast to-
1500Z	+ 34	- 5	- 39	- 45	ward inflection
12 Mar.	+ 27	0	- 36	- 56	point
to 0300Z	- 76	- 62	+ 38	+ 45	
13 Mar.	- 130	- 43	+ 97	+ 23	From inflec-
1954	- 65	- 10	+ 24	+ 29	tion point
	- 82	0	+ 34	+ 27	northeast to-
	- 67	+ 18	+ 41	+ 31	ward ridge
	+ 10	+ 59	+ 47	+130	From inflec-
	- 150	+ 25	+ 64	+ 80	tion point
	- 120	0	+ 57	+ 62	southeast to-
	- 57	- 6	+ 16	+ 31	ward trough
0300Z	- 21	+ 77	- 83	- 150	From trough
to	- 84	- 37	0	- 27	northeast to-
1500Z	+ 11	- 25	- 20	- 42	ward inflection
13 Mar.	+ 23	- 5	- 10	- 18	point
1954	- 150	- 72	+ 85	+ 110	From inflec-
	- 100	- 16	+ 38	+ 42	tion point
	- 85	- 15	+ 39	+ 31	northeast to-
	- 53	- 23	+ 44	0	ward ridge
	- 18	- 31	0	- 11	

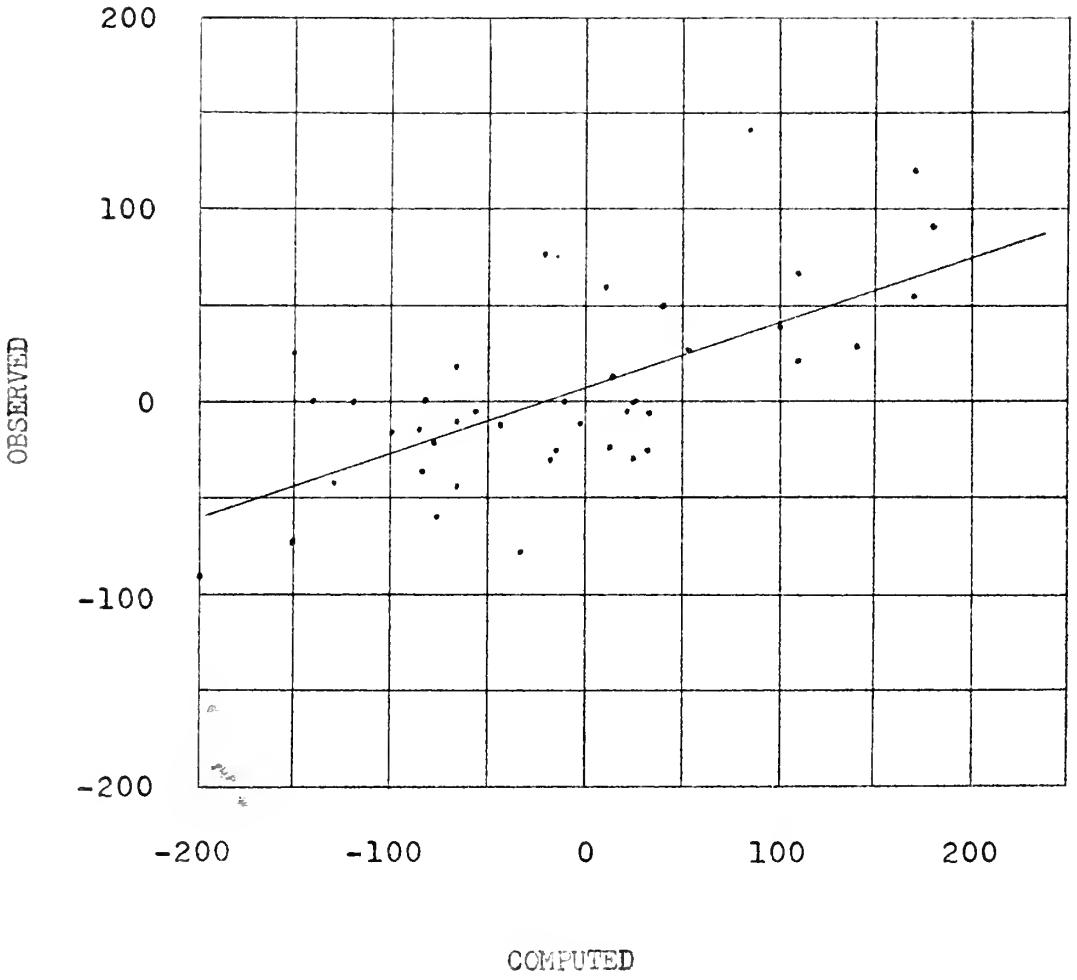

Figure 4. Scatter Diagram and Regression Line of Computed against Observed Normal Isallohyptic Ascendant.

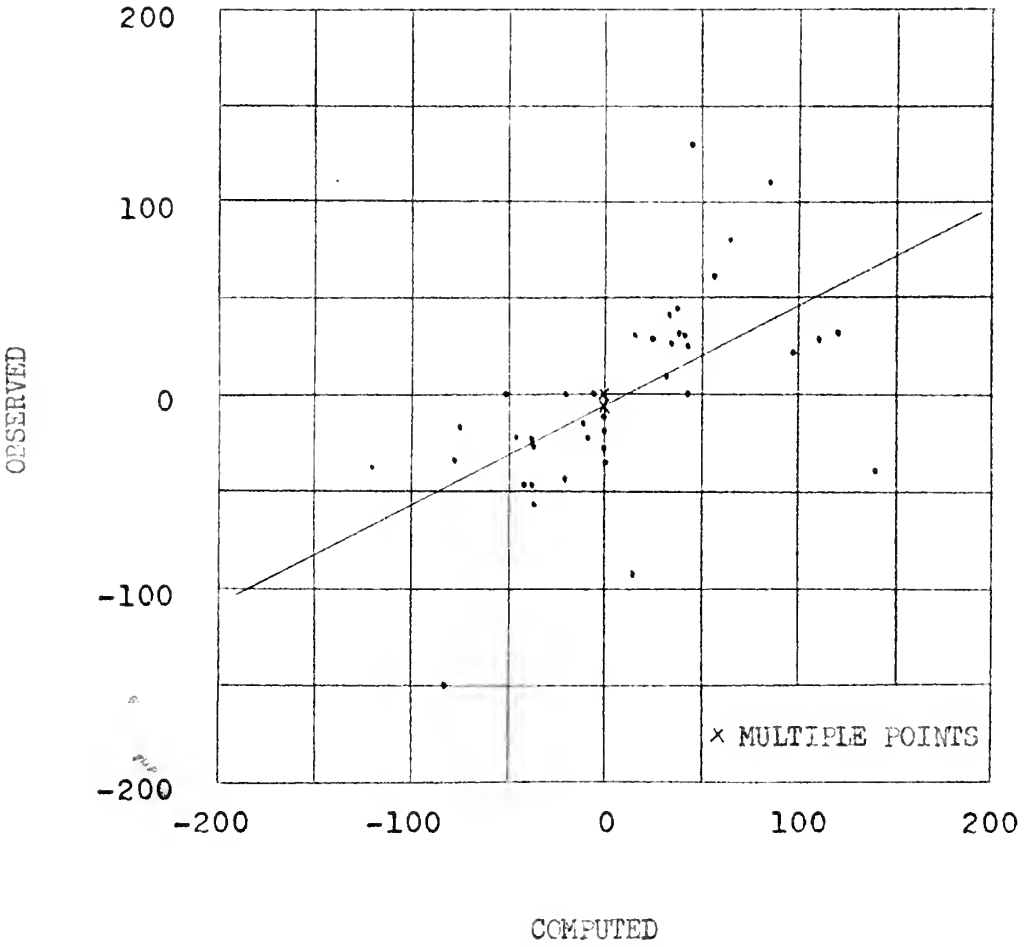

Figure 5. Scatter Diagram and Regression Line of Computed against Observed Tangential Isallohyptic Ascendant.

TABLE 2

Components of Isallohyptic Ascendant Associated with CAVT's Constructed from Isotach Maxima on a 500 Mb. Chart

Date and Time	Isallohyptic Ascendant (feet per deg lat per 12 hrs)				Remarks*
	Normal Component		Tangential Component		
	Computed	Observed	Computed	Observed	
1954					
3/9-03	- 40	- 5	+ 4	+17	Infl. to tr.
3/9-15	- 170	0	+24	0	Near infl. to rdg.
3/10-03	- 3	+ 10	0	+ 29	Rdg. to tr.
3/10-15	- 33	- 40	+ 34	+17	Infl. to tr.
3/11-03	- 210	+ 38	+160	+43	Tr. to. infl.
3/11-15	+ 28	+ 14	- 9	+ 14	Rdg. to. tr.
3/11-15	- 280	+ 45	+ 23	+ 40	Tr. arnd. top of low
3/12-03	- 180	- 100	0	+ 46	Tr. arnd. top of low
3/12-15	- 170	0	0	+ 25	Tr. arnd top of low
3/13-03	- 160	+16	+ 200	+ 9	
4/10-15	- 130	- 20	+ 43	- 33	Tr. to. infl.
4/11-03	- 370	0	+ 230	0	Tr. to. infl.
4/13-03	+ 33	- 8	+ 13	+ 46	Infl. to. tr.
4/14-15	- 6	+ 20	+ 30	- 17	Tr. to. rdg.
4/15-03	+ 41	- 23	- 8	- 14	Infl. to. tr.
4/15-15	+ 190	- 17	- 150	- 54	Near infl. to tr.
4/16-03	+ 150	+150	- 68	- 19	Infl. to tr.

TABLE 2
(Continued)

Date and Time	Isallohyptic Ascendant (feet per deg lat per 12 hrs)				Remarks*
	Normal Component		Tangential Component		
	Computed	Observed	Computed	Observed	
1954					
4/16-15	+180	−56	−210	−12	Infl. to tr.
4/17-03	−180	+140	+110	+12	Near tr. to rdg.
4/17-15	+ 95	− 95	+ 115	+ 87	Infl. acr. wk. rdg. and tr.
4/18-03	+ 120	− 40	0	0	Wk. tr. acr. wk. rdg. and str. tr.

*Abbreviations used in this column are: Infl. inflection point, tr. trough, rdg. ridge, wk. weak, str. strong, arnd. around, acr. across, to. toward.

As in the case of the normal component, this indicates that computed values were predominately of the right sign, but of too great magnitude.

Of the set of 21 trajectories which were constructed from isotach maxima, less than half resulted in computed normal components of the right sign. Also, as may be observed from Table 2, the magnitude of the computed values were almost invariably larger than the magnitude of corresponding observed values.

The correlation coefficient between observed and computed values is -0.09, which is not significant at any acceptable level of belief.

The computed tangential components resulting from this set of 21 trajectories were somewhat better than the computed normal components. These (Table 2) were found to have a correlation coefficient of +0.41 with observed values. This is significant at the 93% level of belief. Since it indicates that the computed values account for only 17% of the variation occurring in the observed data, it cannot be considered a good forecast tool. In this case, as in the others, the magnitude of the computed values was too large. No regression equation was developed for either of the components computed from this series of trajectories.

Because of the large contribution made by the cross-contour term in most of these computations, the CAVT's were examined to try to determine what might be done to the trajec-

tory to reduce this contribution. Usually, though not always, a reduction of the initial wind speed would have resulted in a decrease in the contribution of the first term of (4.4), without changing appreciably the contribution due to the other terms. This might have improved the over-all results; however, more study is required before a definite statement can be made in this regard.

In using the difference equations, (4.4) and (4.5) instead of the differential equations, (2.9) and (2.10), it is assumed that the differences are small enough so that the difference equations closely approximate the integrated forms of the differential equations. This assumption is almost surely not valid when the time interval is 12 hours. Even with a perfect 12-hour trajectory, the results would be somewhat uncertain because of this.

Another source of error is found in the crudeness with which the basic data must be obtained. Curvature plays an important part in this problem in several ways; yet it is difficult to determine the curvature of the contours on an upper air chart with any degree of accuracy. The curvature of the air trajectory is even less attainable. Other parameters are equally difficult to evaluate. This is especially so in connection with short waves for which the measurement of the initial parameters becomes increasingly critical. This presumably accounts for some of the lack of agreement of Table 2. Furthermore, very severe verification criteria were imposed:

The computed normal isallohyptic component was verified along a curve roughly orthogonal to the center point of the various CAVT's. It is quite possible that only a slight displacement of the forecasted isallohyptic centers located by the computational procedure would lead to the variation between the observed and computed isallohyptic gradients. The best test of the 12-hour forecast procedure would be to integrate the isallohyptic tendency equations to determine the complete forecast isallohyptic pattern, and then verify the location of rise and fall centers against the observed pattern. The forecasted isallohyptic gradients correlate sufficiently well (see Chapter V) with the observed gradients, in spite of the severe verification just mentioned.

In certain of the cases presented in Table 2, the CAVT frequently was constructed from a minor trough or ridge or an inflection point between minor features. In such cases, the CAVT frequently crossed a synoptic feature such as a ridge (or trough), continuing right on part way across the next trough (or ridge) downstream. Trajectories of this type may be relatively unrepresentative. The best test in such cases, also, would be that of verification of the forecast isallohyptic patterns.

CHAPTER V

CONCLUSIONS

In Chapter III it was shown that intensification of certain synoptic models on an isobaric surface can be determined qualitatively, provided the required parameters are determinable. Of the parameters required, the most difficult to determine are the cross-contour flow and the local time rate of turning of the wind. The cross-contour flow is by far the more important of these two parameters when using (2.6) or (2.9) with trajectories as drawn in this dissertation.

O'Connor's hypothesis [6] seems to indicate that the most important term in (2.6) is the second term on the right-hand side, since his discussion points out, primarily, those features associated with term B. This follows since O'Connor's point of view is that an isotach maximum or minimum will remain within its appropriate contour channel at each stage of its movement. Thus, no cross-contour flow occurs in this scheme. Furthermore, in many cases, O'Connor's method seems to give acceptable qualitative results.

With the type of trajectories used in this work, the verification was also quite good, at least in the data of Table 1. As discussed in the next paragraph, the cross-contour term A is, in general, much larger than the longitudinal wind difference, term B, and the former gives an over-estimate (with correct sign) of the normal component of isallohyptic

gradient. Thus, the particular objective technique employed herein, while demonstrating the importance of term A, appears to over-estimate it and under-estimate term B. Both of these shortcomings might well be overcome by extracting data from a forecast map halfway through the forecast period. This would have required application of an iterative forecast procedure involving time intervals of 1 - 2 hours at a step. However, the scope of the present work was to devise an objective forecast procedure using only the initial map.

Some information concerning the relative importance of the various terms of (2.9) may be gained by further study of the more successful series of computations, the 44 which are summarized in Table 1. The average contribution of each of the terms (averaged without regard to sign) are: term A (cross-contour term) 73.4, term B (longitudinal wind difference term) 5.7, term C 2.2. The fourth term was ignored because it was small compared with the other terms. The average observed value is 34.8, and the average total computed value is 78.1. Further, the coefficient of correlation between the values of the first term alone and the observed values is +0.55. This is significant at the 99% level of belief. The coefficient of correlation between the second term values and the observed values is -0.03. This is not significant at any acceptable level of belief. Also not significant is the -0.04 correlation coefficient between the computed values of terms A and B.

Although terms B and C of (2.9) are small, there is some improvement in the correlation between observed and computed values when they are included. The discussion at the beginning of this chapter seems to indicate that there must be a certain correspondence between the signs of the first and second terms. Thus, if the second term contribution can be used to indicate the sign of the entire computed value, even though its value is only a small fraction of the total value, it should have the same sign as the contribution from the first or largest term. This is not borne out by the data of this series. Of the 44 pairs of values obtained by matching corresponding terms A and B, there were 38 pairs having non-zero second term values. These 38 pairs consisted of 20 pairs having opposite sign and 18 pairs having the same sign. This lack of correspondence of signs is also indicated by the -0.04 correlation coefficient between these values.

In conclusion it appears that, while significant results have been obtained by using CAVT's drawn from selected points, some more reliable method of determining air trajectories is necessary to make this method a really useful prognostic tool. The evaluation of all terms of (2.9) and (2.10) is dependent on an accurate air trajectory, but it is in the evaluation of term A of (2.9) that trajectory errors are most keenly felt. Without actually constructing trajectories, however, some information can be obtained by qualitative application of the principles which have been set forth. The examples discussed

in Chapter III represent synoptic patterns which are amenable to qualitative interpretation.

BIBLIOGRAPHY

1. Bjerknes, J. Extratropical Cyclones. Compendium of Meteorology, Boston, American Meteorological Society, 1951, p 577-599.

2. Brunt, D. Physical and Dynamical Meteorology, Cambridge, Cambridge University Press, 1939.

3. Cahn, A. J. An Investigation of the Free Oscillations of a Simple Current System. Journal of Meteorology, Vol. 2, No. 2, p 113-119.

4. Hoel, P. G. Introduction to Mathematical Statistics, New York, John Wiley and Sons, Inc., 1947, p 88-89.

5. Martin, F. L. Personal communication during the course of this study. U. S. Naval Postgraduate School, Monterey, California, March 1954.

6. O'Connor, J. F., Lcdr. U.S.N.R. Practical Methods of Weather Analysis and Prognosis, Nav Aer 50-110R-51, p 79-83.

7. Petterssen, S. Weather Analysis and Forecasting, New York, McGraw-Hill, 1940.

8. Rossby, C.-G. On the Mutual Adjustment of Pressure and Velocity Distributions in Certain Simple Current Systems. Sears Foundation Journal of Marine Research, Vol. 1, 1937-38, p 15-28, 239-263.

9. Scherhag, R. Neue Methoden der Wetteranalyse und Wetterprognose, Springer-Verlag, Berlin, 1948, p 156.

APPENDIX I

A METHOD OF CONSTRUCTING CAVT'S FROM ANY POINT

After making the usual assumptions (i.e. non-divergence, constant lateral shear, horizontal frictionless motion), the absolute vorticity equation may be written

$$\frac{V_o}{R_o} + f_o = \frac{V}{R} + f \qquad (1)$$

The subscripts indicate initial conditions.

Subject to the usual additional assumption that V is constant, R may be determined at any latitude for a given set of initial conditions. Thus

$$R = \frac{V}{f_o - f + \frac{V}{R_o}}$$

or

$$R = \frac{V}{2\Omega(\sin\varphi_o - \sin\varphi) + \frac{V}{R_o}} .$$

Substituting appropriate constants and conversion factors to permit the use of V in knots and R_o and R in degrees latitude changes this to

$$R = \frac{V}{31.4(\sin\varphi_o - \sin\varphi) + \frac{V}{R_o}}$$

Radii may be computed for the desired latitudes (either higher or lower than the initial latitude, depending on the initial wind direction). Successive arcs of circles drawn end on end using appropriate radii result in the CAVT. A CAVT constructed by this means is not a curve of continuously

varying curvature. By increasing the number of arcs used in constructing the CAVT, it may, however, be made to approach as closely as is desired the "true" CAVT which has continuously varying curvature. Generally, the computation of radii at 5 degree latitude intervals is adequate.

Figure 6 illustrates the actual CAVT construction process. It is to be noted that the center of curvature of each successive arc lies on a line drawn through the starting point of the arc and the center of curvature of the last arc. This insures continuity of the curve between arc segments. Table 3 lists the initial and computed data used in the CAVT construction shown in Figure 6.

TABLE 3

Initial and Computed Data Used in CAVT Construction Shown in Figure 6

ϕ_o deg	V knots	ψ_o deg	R_o deg lat	$\frac{V}{R_o}$	ϕ deg	$31.4(\sin\phi_o - \sin\phi) + \frac{V}{R_c}$	R deg lat
36.5	85	15	6.0	14.2	37.5	13.8	6.2
					42.5	11.7	7.3
					47.5	9.7	8.8
					52.5	8.0	10.6

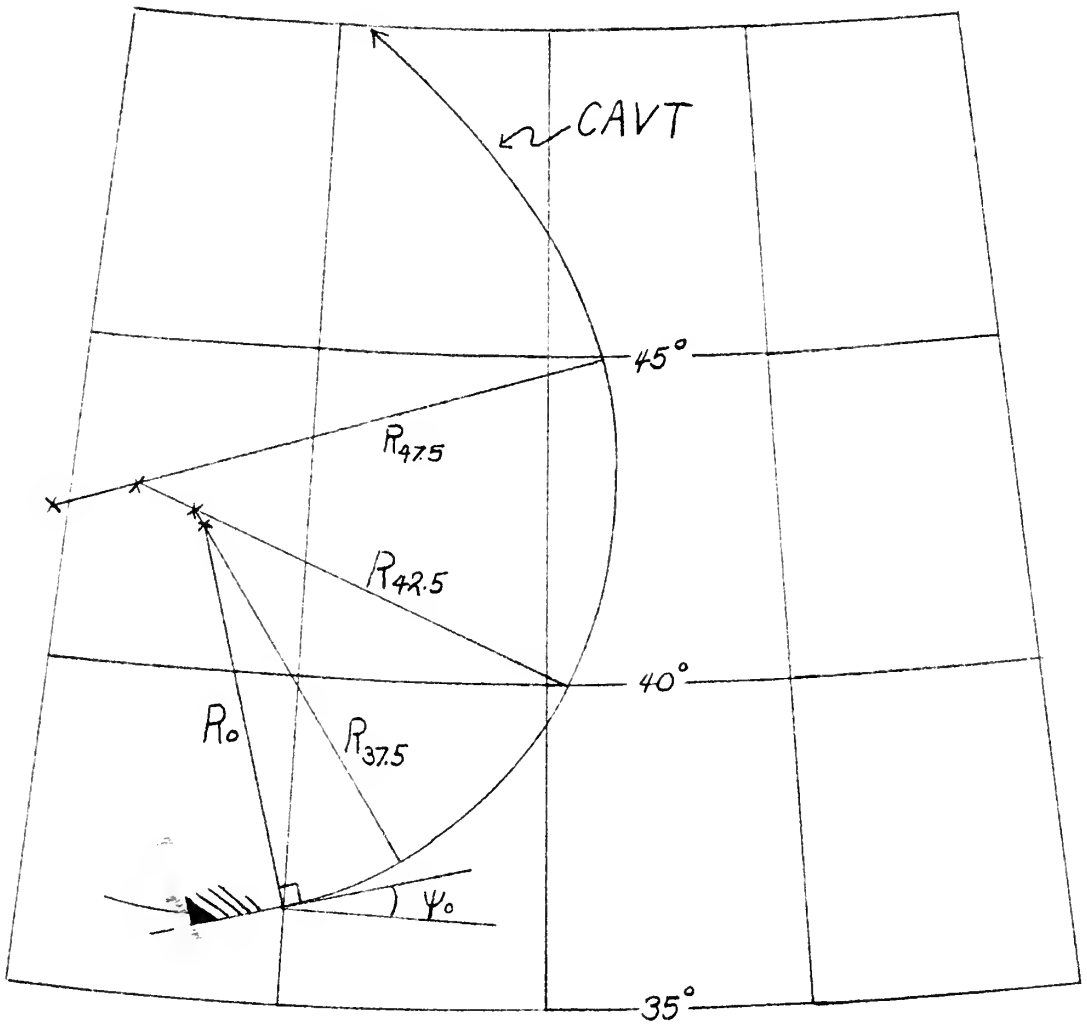

Figure 6. Constructing a CAVT from a Point Other Than an Inflection Point.